

Chapter – 6

Measurement of (n, p) cross section for some structural materials at

14.2 MeV

- 6.1 Introduction
- 6.2 Structural materials for nuclear reactor
- 6.3 Experimental
 - 6.3.1 Target preparation and irradiation
 - 6.3.2 Data acquisition and analysis
- 6.4 Theoretical Predictions
 - 6.4.1 TALYS – 1.6 Calculations
 - 6.4.2 EMPIRE – 3.2.2 Calculations
- 6.5 Results and discussion
- 6.6 Summary and conclusions

References

Publication related to this chapter:

Nand Lal Singh, **Rajnikant Makwana**, S. Mukherjee, A. Chatterjee “Measurement of (n, p) Cross Section for Some Structural Materials at 14.2 MeV”

Published in: IEEE Conference Proceedings; 2016 17th International Scientific Conference on Electric Power Engineering (EPE)

DOI: <https://doi.org/10.1109/EPE.2016.7521819>

Impact Factor: 5.629

6.1 Introduction

Accurate knowledge of neutron induced reaction cross section is of interest to many areas of applied science and fundamental nuclear physics. These cross sections are important to estimate radiation levels, radiation shielding, and decay heat of materials that have been exposed to radiation fields. Other applications are designing of future fusion reactors, advanced fission reactors, in neutron dosimetry and development of nuclear theory. Structural materials are the base materials of any reactor either fusion or fission. The structural materials should have properties such as high strength, long durability, thermal stability, radiation shielding, less radiation transmutation and minimum activation [1]. As these materials are used for the reactor structure, and the neutrons produced from the fission or fusion mechanisms in a reactor are irradiating these materials. The D-T fusion reaction will produce high energy neutrons of 14 MeV. It is necessary to have all the known cross section for this neutron energy to calculate nuclear activation and transmutation, nuclear heating, nuclear damage. The (n, p) reaction channel easily opens for most of the materials above few MeV because of low threshold. The following reaction cross sections were measured by activation technique; $^{75}\text{As}(n, p)^{75}\text{Ge}$, $^{66}\text{Zn}(n, p)^{66}\text{Cu}$, $^{64}\text{Zn}(n, p)^{64}\text{Cu}$, $^{55}\text{Mn}(n, p)^{55}\text{Cr}$, $^{51}\text{V}(n, p)^{51}\text{Ti}$, and $^{58}\text{Ni}(n, p)^{58}\text{Co}$. The uncertainties arising due to self-absorption and self-scattering effects in the bulk samples and pile up effect in detector have been taken care by simulation method as described in the literature [2]. The literature survey reveals that the neutron induced reaction cross sections for these materials are widely studied using standard activation method and are available in EXFOR database [3]. There are large discrepancies among the previous experimental data by a factor of 1.4 to 4.0, hence further measurements are required. The measured cross sections are important for the fusion reactor as well as for the advanced accelerator based sub-critical system. Theoretical evaluation of (n, p) and (n, α) reaction cross sections are done using standard nuclear modular codes, TALYS – 1.6 and EMPIRE – 3.2.2. The predictive power of nuclear reaction models can be validated and improved in comparison with good quality experimental data and in turn, the model calculation provides estimates where no experimental data are available.

6.2 Structural materials for nuclear reactor

The structural materials play a crucial role in designing of a nuclear reactor [4]. It must have properties of long durability and radiation hardness in the radiation environment. The first wall, divertors, breeding blanket, limiters are the component which will face high energy neutrons from the DT fusion [4]. Their properties of mechanical and thermal strength are based on their ability to resist the neutron radiation transmutation. The prime importance of the development of new shielding materials is to develop a material with low activation production in high neutron exposure. In a fission reactor, it is also very necessary to develop new reactor structural materials in order to build new generation upgraded reactors with long durability. The structural materials used in the ITER fusion reactor design are given in FIG 6.1 [5]. The transition metals such as V, Mn, Ni, Zn are always used as a part of the composition of structural materials [6,7]. These materials provide the basic properties such as mechanical strength to the structural composites. The rareearth elements are always present as impurities as well as used with structural materials to enhance its properties [8]. These materials are continuously getting irradiated by neutrons in fusion and fission reactor. The reaction channels such as (n, p), (n, 2n), (n, α) become very important as they can transmute the natural isotopes of these materials into radioactive isotopes. As discussed in earlier chapters, the transmuted isotopes contain different structural properties. Further, the production of long lived radioactive isotopes is a serious problem to the radiation safety and nuclear reactor life. In order to select proper materials for reactor design, it is necessary to have nuclear data for all the structural materials at all the energies in the range of thermal to 20 MeV [8]. It is necessary to have data at 14 MeV for the fusion reactor structural materials. Such effort has been made in the present work for the isotopes of transition metals V, Mn, Zn, Ni and rare earth element As. Arsenic (As) becomes important material as it is used in the production of N – type semiconductors employed in digital electronics, which is part of different electronic components of the reactor. Hence, nuclear transmutation may change its composition and it can offer a change in the electronic response. With these considerations, present measurements become very important.

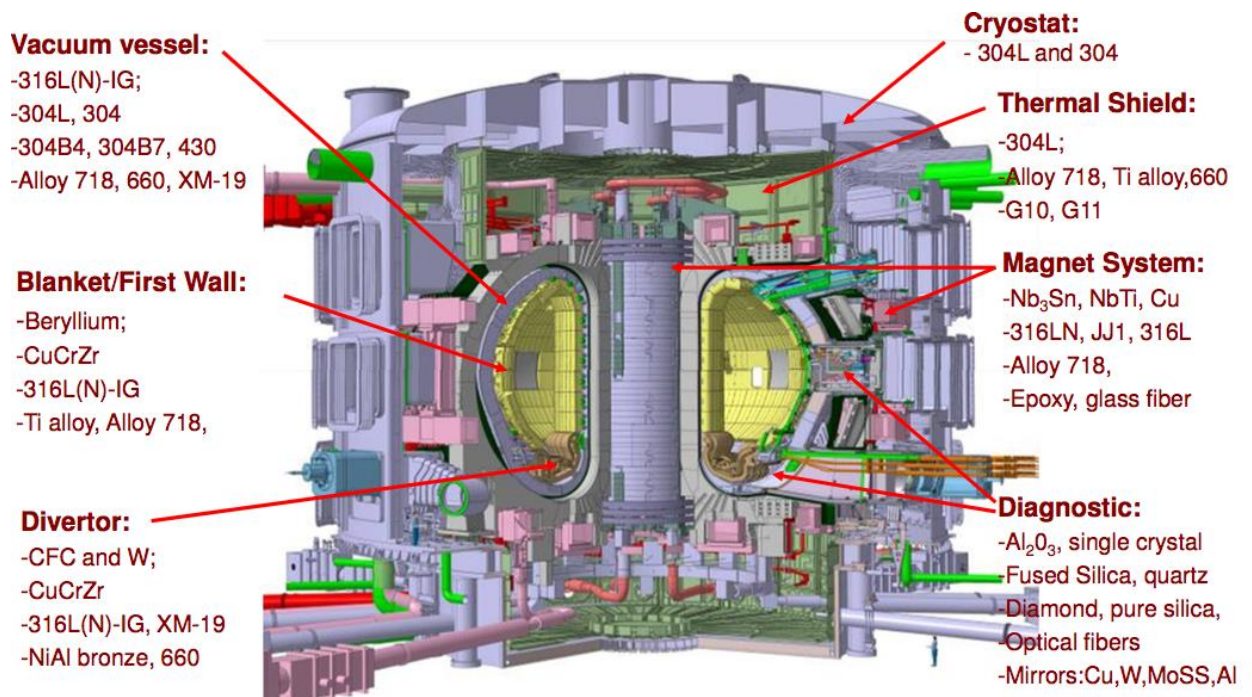


FIG 6.1 The structural materials used in ITER

6.3 Experimental

6.3.1 Target preparation and Irradiation

The target materials in powder form (^{75}As , $^{64,66}\text{Zn}$, ^{55}Mn), were uniformly mixed with aluminum powder and pressed into the form of a pellet of diameter 2.0 cm and thickness of about 2.0 mm each. Four to five pellets were prepared and used as a cylindrical experimental target. The mass of the aluminum and target was measured before addition. The aluminum was used as a monitor to measure the fast neutron flux, incident on the target.

The AN-400 Van de Graff Accelerator of Banaras Hindu University, Varanasi, India was used to produce 14 MeV neutron via $^3\text{H}(d, n)^4\text{He}$ reaction (DT reaction) using tritium target of 8 Ci activity and deuteron beam of energy ~ 280 keV. In this source, deuterium ions are extracted as a beam using the beam extracting system. Once the beam of the deuterium ions is formed, it is accelerated using the 400 keV Van de Graff accelerator. The energy of the ions must be reached such that they can overcome the Coulomb barrier of the tritium nuclei located on target. The beam exposed on the front side of the tritium target which can generate heat. The tritium target is such that the tritium on a titanium metal is continuously cooled through the

passing of cooled water from the back side. The DT source is a mono energetic neutron source, hence it is easy to measure the cross section at DT fusion neutrons energy. Further, the DT neutrons are having energy 14.2 MeV, which is much above the threshold of the presently selected reactions. Hence the considerable amount of activation was expected from the irradiation. In the case of nickel and vanadium instead of pellets, a stack of alternative Ni/V and Al foils were used as a target. These isotopes were irradiated with a beam current of 30 μ A for 15 minutes to 4 hours as per the half-life of product isotope produced in the reaction.

6.3.2 Data acquisition and Analysis

A high purity germanium (HPGe) detector was used for the measurements of activation produced in the irradiated samples. A ^{152}Eu disc source of the same diameter of samples was placed between the sample pallets at different positions. Gamma spectrum at each position was measured with high resolution HPGe detector (1.8 keV FWHM at 1332 keV gamma energy) and 4096 channel multi-channel analyzer. The efficiency of the detector was calculated at different energies of ^{152}Eu with and without a sample to remove self-absorption and self-scattering effects in the samples and pile up effect in the detector as discussed in the literature [2] and is shown in FIG 6.2 for nickel and zinc oxide. It reveals that the percentage attenuation varies nearly 22% to 2.3% for ZnO and 16% to 1.9% for Ni sample for low energy (122 keV) to high energy (1408 keV) gamma rays respectively. The reaction products were identified by means of their characteristics gamma rays and half-life as listed in Table 6.1 [9]. The gamma spectra were measured for each sample using the above mentioned detector setup. As the half-lives of the various product isotopes are different, hence the irradiations were done from minutes to hours accordingly. Those reaction products whose half-lives are in minutes were measured just after the irradiation, with minimum cooling time. The counting were done for several half-lives. A typical gamma spectra from irradiated As the sample is given in FIG 6.2. The analysis was done using neutron activation analysis method as described in the Chapter – 4. The neutron fluxes incidents on the targets were measured by using the Al powder, which was used in the preparation of the target pallets. Al is suitable to measure the flux of high energy neutrons, as the reactions $^{27}\text{Al}(n, \alpha)^{24}\text{Na}$ and $^{27}\text{Al}(n,$

p)²⁷Mg have high threshold energy. Also, ²⁷Al is the only stable and 100% abundant isotope of aluminum [9]. The spectroscopic data for these monitor reactions are given in Table 6.2 [9-15]. Also, the accelerator based DT sources are providing a very small broadening of the neutron energy peak in the front direction [16,17]. The targets and the monitor foils were kept in the front directions with this consideration. The energy of the neutrons was taken as 14.2 ± 0.2 MeV. The cross section was calculated from the measured photopeak counts using the following activation eq. 6.1. The measured cross sections are given in Table 6.3.

$$\sigma = \frac{A_i A_\gamma \lambda e^{\lambda t_w}}{\phi \theta_\gamma P_\gamma w_i P_i N_{av} (1 - e^{-\lambda t_i})(1 - e^{-\lambda t_c})} \quad 6.1$$

where,

A_i = Gram Atomic Weight of the target

A_γ = Peak Counts of gamma energy

λ = Decay constant of the product isotope

t_i = irradiation time

t_w = Cooling time

t_c = Counting time

ϕ = Incident neutron flux

θ_γ = Efficiency of detector at gamma chosen

P_γ = Gamma intensity

w_i = Weight of the sample

P_i = Abundance of the target isotope

N_{av} = Avogadro's number

Table 6.1 Selected nuclear reactions with their product isotope, half-life and prominent gamma ray energies with intensities

Target isotope with abundance	Nuclear reaction	Product Isotope (Half-life) [9-15]	Prominent Gamma ray energy (keV) with gamma intensity [9-15]
⁷⁵ As (100%)	⁷⁵ As(n, p) ⁷⁵ Ge	⁷⁵ Ge (82.78 m)	264.65 (11%)
⁶⁶ Zn (27.73%)	⁶⁶ Zn(n, p) ⁶⁶ Cu	⁶⁶ Cu (5.120 m)	1039.23 (9.23%)
⁶⁴ Zn (49.17%)	⁶⁴ Zn(n, p) ⁶⁴ Cu	⁶⁴ Cu (12.7 h)	1345.84 (0.475%)
⁵⁵ Mn (100%)	⁵⁵ Mn(n, p) ⁵⁵ Cr	⁵⁵ Cr (3.497 m)	1528.3 (0.037%)
⁵¹ V (99.75%)	⁵¹ V (n, p) ⁵¹ Ti	⁵¹ Ti (5.76 m)	320.07 (93.1%)
⁵⁸ Ni (68.077%)	⁵⁸ Ni(n, p) ⁵⁸ Co	⁵⁸ Co (70.86 d)	511 (29.8%); 810.76 (99.45%)

Table 6.2 The Monitor reactions used for neutron flux measurements

Monitor Nuclear reaction	Product Isotope (Half-life) [9]	Prominent Gamma ray energy (keV) with gamma intensity (%) [9]
²⁷ Al(n, α) ²⁴ Na	²⁴ Na (14.96 h)	1368.6 (100)
²⁷ Al(n, p) ²⁷ Mg	²⁷ Mg (4.46 m)	843.8 (71.8)

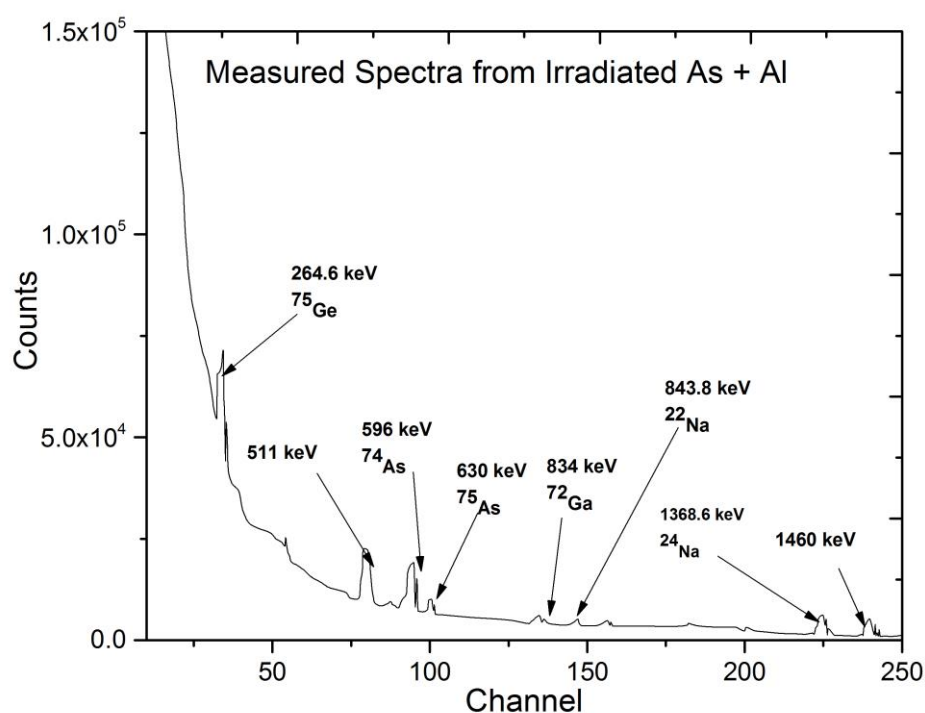


FIG 6.2 Typical measured gamma spectra from irradiated mixed powder of (As_2O_3 , + Al) using HPGe detector

6.4 Theoretical Predictions

The nuclear modular codes are an important tool for the calculation and verification of the cross sections of various nuclear reactions at a different incident energy of the projectile. The latest version of nuclear modular codes TALYS-1.6/1.8 and EMPIRE-3.2.2 are used to evaluate (n, p) cross sections for the selected isotopes [18, 19]. The input parameters such as level density parameter have been precisely chosen for best estimation of the cross section. The details of these parameters have been already discussed in Chapter – 2.

6.4.1 TALYS-1.6 Calculations

TALYS is a computer code which is efficient to predict nuclear reaction cross section. It is a useful tool to do analysis of physics of nuclear reactions. TALYS – 1.6 nuclear code can calculate cross section for incident particles; gammas, neutrons, protons, deuterons, tritons, ³He and alpha-particles in the incident energy range from 1 keV to 200 MeV for target nuclides of mass 12 and heavier nuclei. TALYS

considers all the possible channels for the above-mentioned particles. It has completely integrated optical model and Coupled-channels calculations by ECIS-06 code [20]. The optical model parameters are used for neutron and photon reaction calculations determined from global potential proposed by Koning and Delaroche [21]. The compound model contribution is developed from Hauser-Feshbach model [22]. The pre-equilibrium calculation is developed from the exciton model proposed by Kalbach [23]. In this calculation, pre-equilibrium effect is considered as default parameters.

6.4.2 EMPIRE – 3.2 Calculations

EMPIRE – 3.2 is another powerful nuclear modular system to predict nuclear reaction cross section. It considers reaction mechanism such as compound nucleus formation (Hauser-Feshbach model) with width fluctuation correction [22,24], pre-equilibrium using exciton model and direct reaction using the optical model parameters given in RIPL – 3 library. The present version of the EMPIRE code is the latest version. EMPIRE makes use of several codes, written by different authors, which were converted into subroutines and adapted for the present use [25]. For the present work, the level density parameter was changed to get the best agreement with the measured data (Level density parameter for EGSM, Gilbert-Cameron (EMPIRE) and GSM (RIPL) models [26,27]).

Both the codes were used to calculate cross section for the selected reactions and are plotted in the **FIGS. 6.4 – 6.9** along with the previous data. There is a fairly good agreement between present measured data with those of calculated data using TALYS-1.6 and EMPIRE-3.2.2. The present experimental result and theoretical predictions using above codes are also listed in **Table 6.2**.

6.5 Results and discussion

The cross sections were measured with improved accuracy using the simulation method, which takes care of self-absorption and self-scattering effects in the samples and pile up effect in the detector. The errors quoted on the cross section comprise the statistical error (1-3%), relative efficiency (2-3%) and the monitor cross section (3%). The relative efficiency data with and without absorber for a particular

target-detector geometrical arrangement inclusive of all due to self-scattering, self absorption and geometrical solid angle for a cylindrical target was used to determine cross section, such curve for nickel and zinc oxide is presented in FIG 6.3. The present experimental results are compared with the available experimental data from EXFOR database [3] and evaluated with Talys – 1.6 and EMPIRE – 3.2.2 codes are shown in FIGS. 6.4 – 6.9. The cross section measured in the present work and by others with the same experimental method are in agreement within about 2-15%.

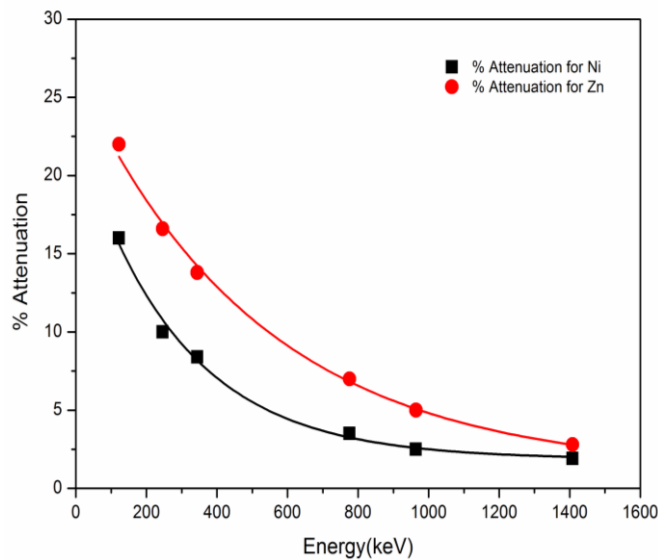


FIG 6.3 Self absorption and self scattering effect for Ni and Zn sample

Table 6.3 Comparison of measured and theoretically predicted cross section data for the present selected reactions

Nuclear Reaction	Measured Cross section (mb) at 14.2 ± 0.2 MeV	Calculated Cross section (mb)	
		TALYS – 1.6	EMPIRE – 3.2.2
$^{75}\text{As}(n, p)^{75}\text{Ge}$	27.2 ± 1.6	25.58	22.44
$^{66}\text{Zn}(n, p)^{66}\text{Cu}$	55.5 ± 3.3	50.72	49.32
$^{64}\text{Zn}(n, p)^{64}\text{Cu}$	170.0 ± 10.2	137.12	176.33
$^{55}\text{Mn}(n, p)^{55}\text{Cr}$	45.8 ± 2.7	26.92	36.23
$^{51}\text{V}(n, p)^{51}\text{Ti}$	28.2 ± 1.7	35.90	30.52
$^{58}\text{Ni}(n, p)^{58}\text{Co}$	314.0 ± 18.8	278.96	263.83

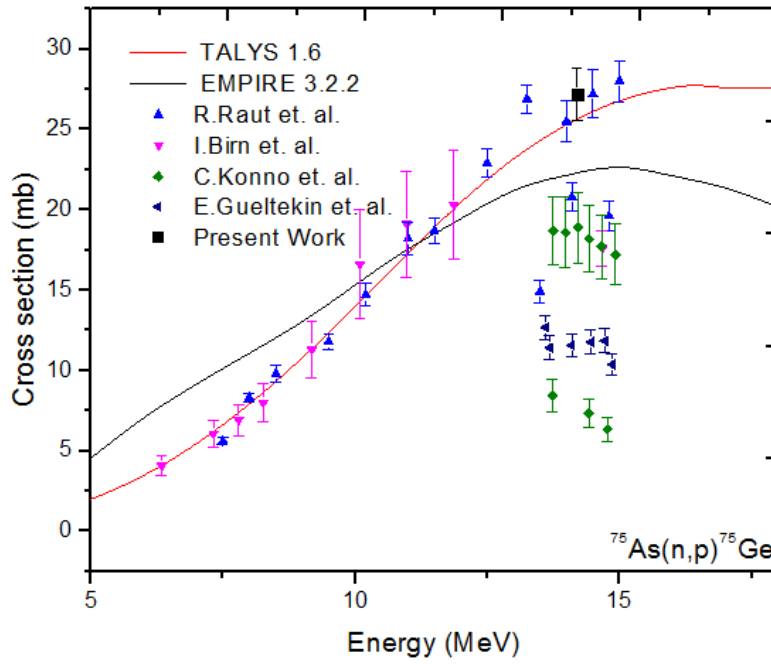


FIG 6.4 Comparison of measured $^{75}\text{As}(n, p)^{75}\text{Ge}$ Cross section with EMPIRE-3.2.2, TALYS-1.6, EXFOR data

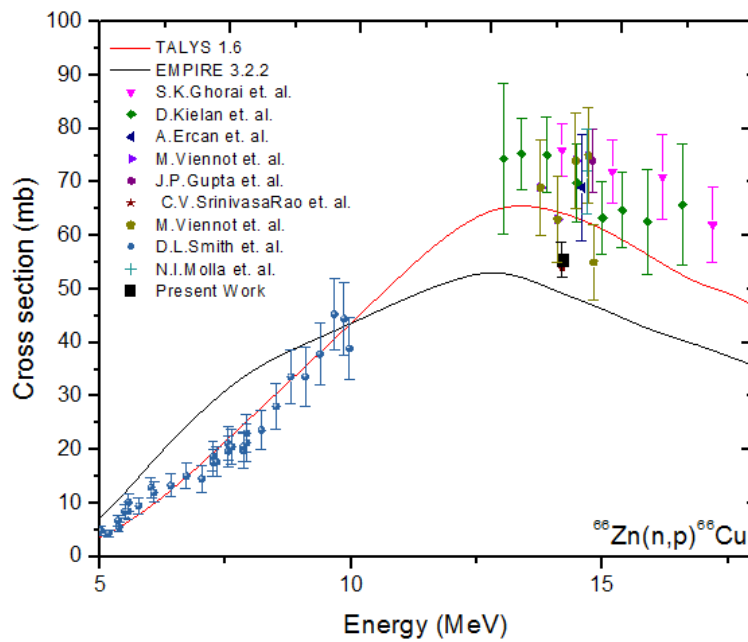


FIG 6.5 Comparison of measured $^{66}\text{Zn}(n, p)^{66}\text{Cu}$ Cross section with EMPIRE-3.2.2, TALYS-1.6, EXFOR data

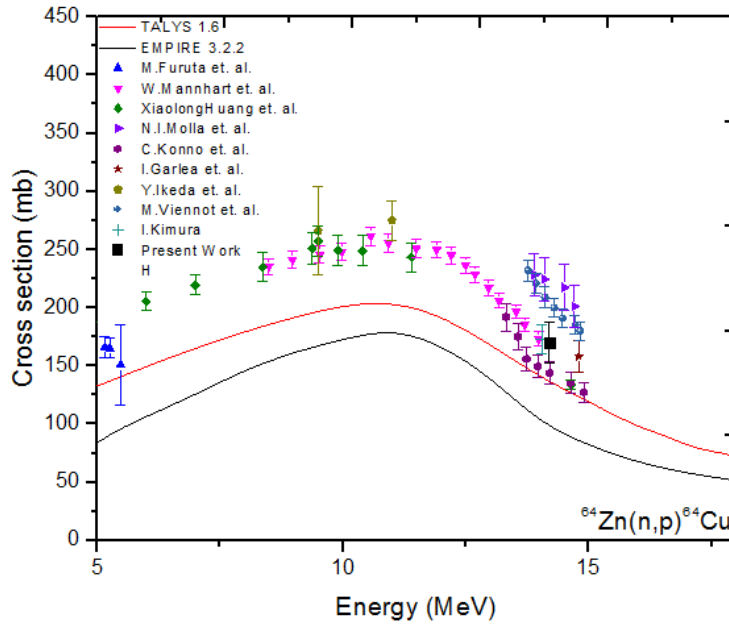


FIG 6.6 Comparison of measured $^{64}\text{Zn}(n, p)^{64}\text{Cu}$ Cross section with EMPIRE-3.2.2, TALYS-1.6, EXFOR data

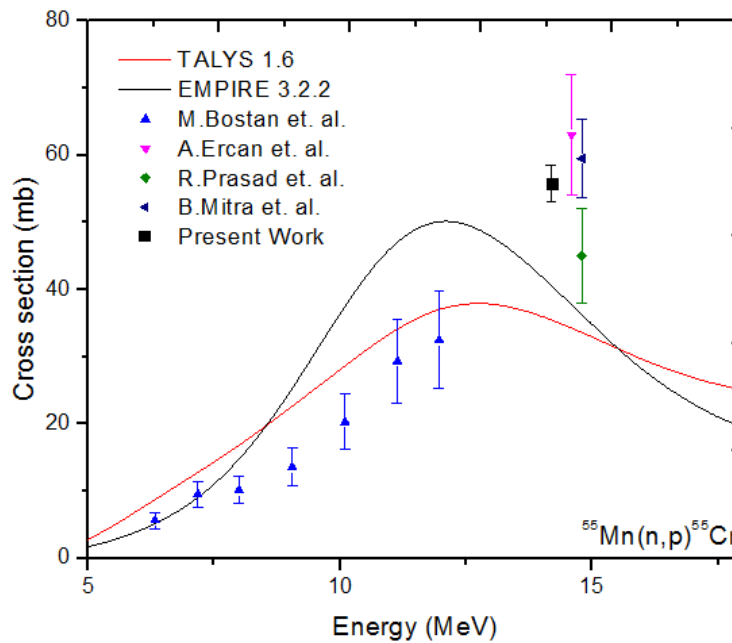


FIG 6.7 Comparison of measured $^{55}\text{Mn}(n, p)^{55}\text{Cr}$ Cross section with EMPIRE-3.2.2, TALYS-1.6, EXFOR data

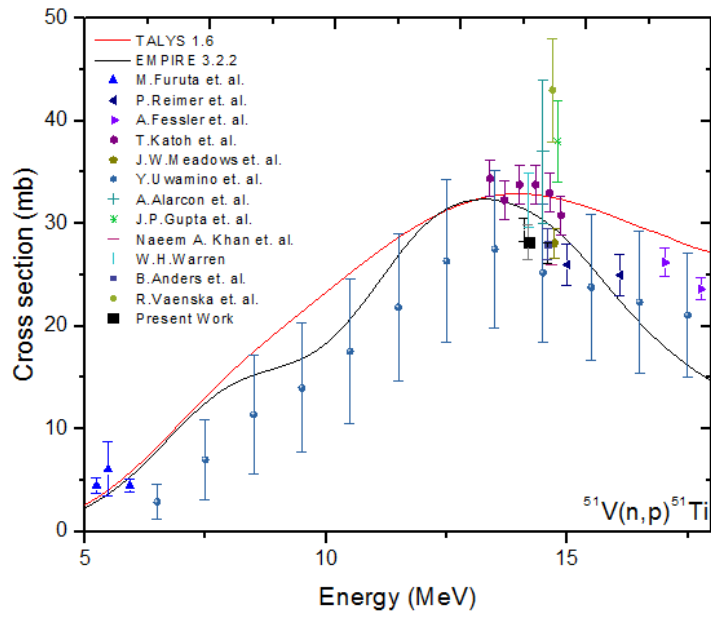


FIG 6.8 Comparison of measured $^{51}\text{V}(n, p)^{51}\text{Ti}$ Cross section with EMPIRE-3.2.2, TALYS-1.6, EXFOR data

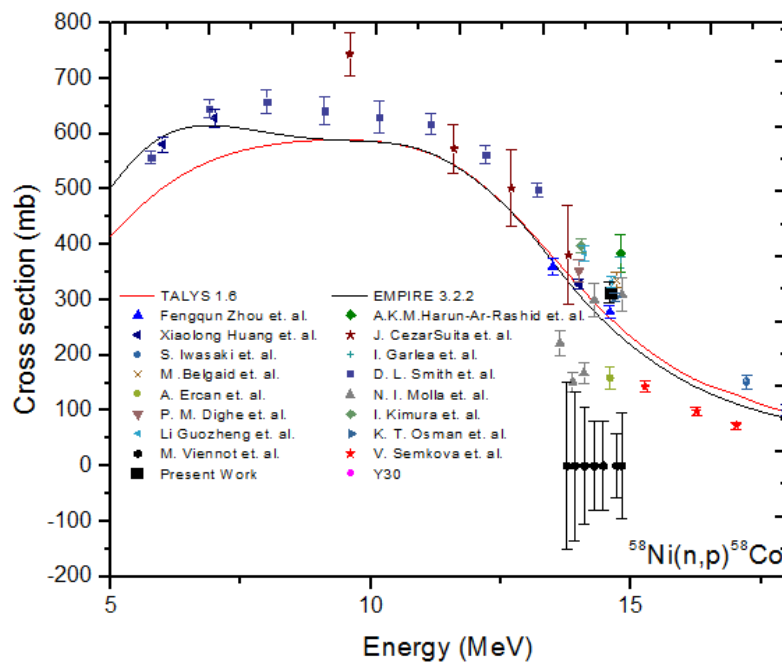


FIG 6.9 Comparison of measured $^{58}\text{Ni}(n, p)^{58}\text{Co}$ Cross section with EMPIRE-3.2.2, TALYS-1.6, EXFOR data

6.6 Summary and conclusions

In the present study, the (n, p) reaction cross sections for some of the structural materials such as ^{75}As , ^{66}Zn , ^{64}Zn , ^{55}Mn , ^{51}V and ^{58}Ni were measured at 14.2 ± 0.2 MeV. The offline gamma spectroscopy and neutron activation analysis method were used for the data analysis. The present results were compared with the previously measured data available in EXFOR database as well as theoretical predictions using code TALYS – 1.6 and EMPIRE – 3.2. Present results are in fairly good agreement with some previous measurements and also with theoretical predictions. The results are important for the DT fusion neutrons as well as for the enhancement of the nuclear data library.

References

- [1] N. L. Singh, et al., Proc. of DAE Sympo. on Nucl. Phys. 59 (2014) 566. ; 60 (2015) 442.
- [2] N. L. Singh, P. M. Prajapati, Electric Power Engineering, 739-742 (2014).
- [3] Experimental Nuclear Reaction Data (EXFOR); <https://www-nds.iaea.org/exfor>
- [4] M. Victoria, N. Baluc and P. Spätig, EPFL-CRPP Fusion Technology Materials, CH-5232 Villigen PSI, Switzerland.
- [5] V. Barabash, First Joint ITER-IAEA Technical Meeting on “Analysis of ITER Materials and Technologies”, 23 – 25 November 2010, Principality of Monaco.
- [6] B. Raj and M. Vijayalakshmi, Joint ICTP/IAEA School on Physics and Technology of Fast Reactors Systems, “Radiation Damage of Structural Materials for Fast Reactor Fuel Assembly (3)”, Strada Costiera, Italy.
- [7] Y. Kasugai, et al., Fusion Engineering and Design 42 (1998) 299–305.
- [8] D. Zhou, P. Peng, S. Xu, J. Liu, Research and application of rare earth in steel. Res. Stud. Foundry Equip. 2004, 3, 35–38.
- [9] NNDC, ENSDF database, <https://www.nndc.bnl.gov/chart/>
- [10] A. R. Farhan, S. Rab, Nuclear Datasheet for A=75, Nucl. Dat. Sheets 60, 735 (1990).
- [11] M. R. Bhat, Nucl. Dat. Sheets 83, 789 (1998).
- [12] Huo Junde, Nucl. Dat. Sheets 64, 723 (1991).
- [13] B. Singh, Nucl. Dat. Sheets 78, 395 (1996).
- [14] R. L. Auble, Nucl. Dat. Sheets 23, 163 (1978).
- [15] C. D. Nesaraja, et al., Nucl. Dat. Sheets 111, 897 (2010).
- [16] M. Pillon, et al., Fusion Engineering and Design 28 (1995) 683-688.
- [17] Guan-bo Wang, et al., <http://dx.doi.org/10.1016/j.nima.2014.04.079>.
- [18] A. J. Koning, et. al., Talys-1.6, A Nuclear reaction program, user manual, NRG-1755 Z. G. Petten, Netherlands(2011)
- [19] M. Herman, et. al., EMPIRE-3.2.2 modular system for nuclear reaction calculations and nuclear data evaluation User's Manual
- [20] J. Raynal, Notes on ECIS94, CEA Saclay Report No. CEA-N-2772, (1994).

- [21] A. J. Koning, J. P. Declaroche, Nucl. Phys., A713: 231-310(2003).
- [22] W. Hauser, H. Feshbach, Phys. Rev, 87:366(1952).
- [23] C. Kalbach, Phy. Rev. C 33, 818–833 (1986).
- [24] S. Hofmann, et al., Ann. Phys. 90, 403 (1975);
S. Hofmann, et al., Z. Physik A 297,153 (1980)
- [25] A. V.Ignatyuk, J. Nucl Phys. 21, 255 (1975)
- [26] A. Gilbert, et al., Can J. Phys. 43, 1446 (1965)
- [27] S. Hilaire, et al., Nucl. Phys, A779: 63-81(2006).